Electronic Supplementary Material (ESI) for Physical Chemistry Chemical Physics.


# Supporting information for: Amino-Acid Interactions with Au(111) Surface: Adsorption, Band Alignment, and Interfacial Electronic Coupling

Zdenek Futera*

*Faculty of Science, University of South Bohemia, Branisovska 1760, 370 05 Ceske Budejovice, Czech Republic.*

E-mail: zfutera@prf.jcu.cz(Z.F.)

Phone: +420-387-776-254

## BDA on Au(111) surface

To validate our computational setup we first calculated the band alignment correction for 1,4-benzenediamine (BDA) adsorbed on Au(111) slab of the same size as used for the amino-acid calculations. This system was previously experimentally probed by ultraviolet photoemission spectroscopy (UPS) and X-ray photoemission spectroscopy (XPS),[S1] and computationally investigated by many-body GW calculations,[S2] hybrid-functional DFT[S3] as well as by PBE-based DFT+$\Sigma$ approach.[S4,S5] We fully optimized BDA/Au(111) interface at the vdW-DF level and then, for comparison, reoptimized the structure also with PBE functional. The obtained adsorption distances, energies, and band-alignment corrections are listed in Table S1.

Both functionals place the adsorbed BDA molecule in 3.37 Å heavy-atom distance from the Au(111) surface with amino-group hydrogens pointing to the surface. As expected, there is a large difference in adsorption energy predicted by PBE (-0.35 eV) and vdW-DF (-0.94 eV) as the dispersion interactions between the polarizable metal surfaces and aromatic molecules play an important role. On the other hand, vdW-DF predicts practically the same HOMO-LUMO gap of the gas-phase BDA as PBE (3.26 eV vs. 3.21 eV, respectively), which is severely underestimated due to the self-interaction error. The OT-RSH gap is by $\sim$5.5 eV larger reaching the values 8.77 eV (PBE) and 8.78 eV (vdW-DF) where $\omega = 0.237$ Bohr$^{-1}$ parameter found optimal for both functionals was applied. The molecular gap correction $\Sigma_j^0$ shifts the HOMO of the BDA molecule by almost 3 eV to the lower energies while pushing up LUMO by $\sim$2.5 eV.

The interfacial HOMO-LUMO gap of the BDA adsorbed on Au(111) is unchanged in GGA type functionals used here. This is true not only for PBE but also for vdW-DF which improves the adsorption energy but predicts the electronic states consistent with PBE. To determine the interfacial state renormalization we fitted the XC potential above the clean Au(111) surface to the classical image-charge potential $V_{\mathrm{img}}$, as described above. The fit is shown in Fig. S4 where both the XC and $V_{\mathrm{img}}$ potentials are shown. While the surface-plane distance $z_0$ is 0.97 Å for PBE, it is shifted to 1.55 Å in vdW-DF where the XC potential

has a shoulder between 2.2 – 3.5 Å caused by exchange enhancement in this functional. The corresponding surface-plane distance, obtained by common-tangent-point fitting, is rather large and leads to overpolarization as we discuss below.

Here, we compare several approaches to calculate the polarization energy of the molecule on the gold interface. The $V_{\mathrm{img}}$ potential depends only on the distance from the surface. Simultaneously, the molecule lies on the surface with all atoms at a similar adsorption distance, it is sensible to evaluate the polarization at the center of the molecule. The obtained energy is ∼1.5 eV for $V_{\mathrm{img}}$ fitted to XC potential of PBE ($z_0 = 0.97$ Å) predicting the $\Sigma_{\mathrm{HOMO}}$ = -1.5 eV (-1.4 eV) on PBE (vdW-DF) geometry, in good agreement with reference GW and UPS/XPS data.[S1,S2] On the other hand, $V_{\mathrm{img}}$ obtained from XC potential of vdW-DF ($z_0 =$ 1.55 Å) tends to overestimate the polarization energy (2.0 eV) and as a result, predicts the band-alignment correction which is by 0.5 eV smaller in absolute value.

Although the center-point approximation works well for BDA it could not be justified for amino acids, which are not flat and considerable variation in their atomic distances from the surface might be expected, as we show further in this work. In such cases, a set of atomic point charges can serve as a good approximation of the molecule for polarization-energy calculations. As the atomic charges are not unique, we benchmark here three population analyses often used in molecular DFT calculations, namely Mulliken, Lowdin, and Hirshfeld charges. While the first two predict reasonable polarization energies (∼1.6 eV for $z_0 =$ 0.97 Å), the Hirshfeld charges overestimate this energy by 0.4 eV. The effect of larger $z_0$, as obtained for vdW-DF, is enhanced here comparing to center-point approximation because of overpolarization of the atoms closer to the surface and leading to unrealistic polarization as high as 3.0 eV in the case of Hirshfeld charge scheme. On the other hand, Mulliken and Lowdin charges are known to be rather strongly basis set dependent.

To avoid ambiguities with atom-charge assignment we eventually obtained the polarization energy by the integration of HOMO and LUMO orbitals in the $V_{\mathrm{img}}$ potential (c.f. Eq. 7 in the main text). The obtained energy is 1.6 eV, placing the HOMO of BDA to

the correct position with respect to interfacial Fermi level $E_F$ when $z_0 = 0.97$ Å is used. Again, larger $z_0$ leads to overpolatization and underestimates the resulting band-alignment correction by 0.8 eV. Based on these benchmarked data we conclude that the OT-RSH based gap correction together with renormalization correction based on frontier-orbital integration in classical image-charge potential is the optimal DFT+$\Sigma$ setup and therefore we apply it for the band-alignment prediction of amino acids presented in this work.

Table S1: DFT+$\Sigma$ corrections for benzenediamine (BDA) adsorbed on Au(111) surface. OT-RSH range-separation parameter $\omega$ was found 0.2374 Bohr$^{-1}$ corresponding to distance 2.229 Å both for PBE and vdW-DF. Surface plane position $z_0$ of the image-charge potential $V_{img}$ and adsorption distances $d_{ads}$ are given in Å, while the adsorption energies $E_{ads}$, energy HOMO-LUMO gaps $E_g$, corrections $\Sigma_j^0$, $\Sigma_j^{pol}$, $\Sigma_j$, state energies $\epsilon_j$, $\epsilon_{\Sigma_j}$ and Fermi energies $E_F$ are given in eV.

| | | PBE | | vdW-DF($V_{img}^{\mathrm{PBE}}$) | | vdW-DF | |
|---|---|---|---|---|---|---|---|
| | | HOMO | LUMO | HOMO | LUMO | HOMO | LUMO |
| | $z_0$ | 0.97 | | 0.97 | | 1.55 | |
| | $d_{ads}$ | 3.372 | | 3.376 | | 3.376 | |
| | $E_{ads}$ | -0.349 | | -0.940 | | -0.940 | |
| | $E_g$ | 3.208 | | 3.264 | | 3.264 | |
| | $E_g^{\mathrm{OT\text{-}RSH}}$ | 8.774 | | 8.780 | | 8.780 | |
| | $\Sigma_j^0$ | -2.980 | 2.584 | -2.843 | 2.673 | -2.843 | 2.673 |
| | $\epsilon_j - E_F$ | -0.041 | 3.262 | -0.045 | 3.302 | -0.045 | 3.302 |
| Geom center | $\Sigma_j^{pol}$ | 1.532 | -1.532 | 1.530 | -1.530 | 2.031 | -2.031 |
| | $\Sigma_j$ | -1.448 | 1.052 | -1.313 | 1.143 | -0.812 | 0.642 |
| | $\epsilon_{\Sigma_j} - E_F$ | -1.489 | 4.314 | -1.358 | 4.445 | -0.857 | 3.944 |
| Mass center | $\Sigma_j^{pol}$ | 1.491 | -1.491 | 1.486 | -1.486 | 1.953 | -1.953 |
| | $\Sigma_j$ | -1.489 | 1.093 | -1.357 | 1.187 | -0.890 | 0.720 |
| | $\epsilon_{\Sigma_j} - E_F$ | -1.530 | 4.355 | -1.402 | 4.489 | -0.935 | 4.022 |
| Mulliken charges | $\Sigma_j^{pol}$ | 1.678 | -1.387 | 1.663 | -1.399 | 2.274 | -1.797 |
| | $\Sigma_j$ | -1.302 | 1.197 | -1.180 | 1.274 | -0.569 | 0.876 |
| | $\epsilon_{\Sigma_j} - E_F$ | -1.343 | 4.459 | -1.225 | 4.576 | -0.614 | 4.178 |
| Lowdin charges | $\Sigma_j^{pol}$ | 1.620 | -1.398 | 1.621 | -1.391 | 2.197 | -1.783 |
| | $\Sigma_j$ | -1.360 | 1.186 | -1.222 | 1.282 | -0.646 | 0.890 |
| | $\epsilon_{\Sigma_j} - E_F$ | -1.401 | 4.448 | -1.267 | 4.584 | -0.691 | 4.192 |
| Hirshfeld charges | $\Sigma_j^{pol}$ | 2.061 | -0.881 | 2.098 | -0.835 | 3.053 | -0.787 |
| | $\Sigma_j$ | -0.919 | 1.703 | -0.745 | 1.838 | 0.021 | 1.886 |
| | $\epsilon_{\Sigma_j} - E_F$ | -0.960 | 4.965 | -0.790 | 5.140 | -0.024 | 5.188 |
| MO integration | $\Sigma_j^{pol}$ | 1.574 | -1.624 | 1.563 | -1.617 | 2.225 | -2.370 |
| | $\Sigma_j$ | -1.406 | 0.960 | -1.280 | 1.056 | -0.618 | 0.303 |
| | $\epsilon_{\Sigma_j} - E_F$ | -1.447 | 4.222 | -1.325 | 4.258 | -0.663 | 3.605 |

Table S2: PBE gas-phase HOMO-LUMO energy gap corrections for capped amino acids. The gap was calculated on gas-phase geometries optimized by PBE. The range-separation parameter $\omega$ is given in Bohr$^{-1}$, corresponding to a range-separation distance $\rho = 1/\omega$ in Å. $E_g$ denotes the HOMO-LUMO energy gap, $\Sigma^0_{\mathrm{HOMO}}$ and $\Sigma^0_{\mathrm{LUMO}}$ are the energy level corrections for the HOMO and LUMO, respectively, given in eV.

| Amino acid | $\omega$ | $\rho$ | $E_g^{\mathrm{PBE}}$ | $E_g^{\mathrm{OT\text{-}RSH}}$ | $\Sigma^0_{\mathrm{HOMO}}$ | $\Sigma^0_{\mathrm{LUMO}}$ |
|---|---|---|---|---|---|---|
| Ala | 0.2265 | 2.336 | 4.571 | 11.363 | -3.832 | 2.960 |
| Arg | 0.2144 | 2.468 | 4.290 | 10.457 | -3.288 | 2.878 |
| Asn | 0.2153 | 2.458 | 4.604 | 10.912 | -3.501 | 2.807 |
| Asp | 0.2374 | 2.229 | 4.131 | 10.809 | -3.712 | 2.966 |
| Cys | 0.2293 | 2.308 | 4.427 | 10.835 | -3.472 | 2.936 |
| Gln | 0.2131 | 2.483 | 4.582 | 10.992 | -3.588 | 2.822 |
| Glu | 0.2278 | 2.323 | 4.483 | 11.296 | -3.812 | 3.002 |
| Gly | 0.2373 | 2.230 | 4.541 | 11.514 | -3.936 | 3.037 |
| His($\delta$) | 0.2131 | 2.483 | 3.799 | 9.599 | -2.961 | 2.840 |
| His($\epsilon$) | 0.2091 | 2.531 | 4.222 | 10.322 | -3.374 | 2.726 |
| Ile | 0.2167 | 2.442 | 4.507 | 10.853 | -3.503 | 2.844 |
| Leu | 0.2284 | 2.317 | 4.603 | 11.386 | -3.830 | 2.953 |
| Lys | 0.2279 | 2.322 | 4.595 | 11.218 | -3.677 | 2.945 |
| Met | 0.2226 | 2.377 | 4.683 | 10.858 | -3.282 | 2.893 |
| Phe | 0.2051 | 2.580 | 3.982 | 9.868 | -3.372 | 2.513 |
| Pro | 0.2172 | 2.436 | 4.521 | 10.798 | -3.451 | 2.827 |
| Ser | 0.2255 | 2.347 | 4.598 | 11.059 | -3.588 | 2.872 |
| Thr | 0.2374 | 2.229 | 4.639 | 11.282 | -3.669 | 2.974 |
| Trp | 0.2010 | 2.633 | 3.623 | 8.671 | -2.684 | 2.364 |
| Tyr | 0.2010 | 2.633 | 3.726 | 9.295 | -3.103 | 2.465 |
| Val | 0.2176 | 2.432 | 4.520 | 10.881 | -3.515 | 2.846 |
| Average | 0.2202 | 2.409 | 4.364 | 10.679 | -3.483 | 2.832 |

Table S3: PBE intefacial state renormalization determined by image-charge interaction of frontier molecular orbitals of the capped amino acids adsorbed on Au(111) surface. The image-charge energy $\Sigma_j^{pol}$ and the total HOMO / LUMO corrections $\Sigma_{\mathrm{HOMO}}$, $\Sigma_{\mathrm{LUMO}}$ are given in eV.

| Amino acid | $\Sigma_{\mathrm{HOMO}}^{pol}$ | $\Sigma_{\mathrm{LUMO}}^{pol}$ | $\Sigma_{\mathrm{HOMO}}$ | $\Sigma_{\mathrm{LUMO}}$ |
|---|---|---|---|---|
| Ala | 0.999 | -1.386 | -2.833 | 1.574 |
| Arg | 0.852 | -1.435 | -2.436 | 1.443 |
| Asn | 0.936 | -1.468 | -2.565 | 1.339 |
| Asp | 1.429 | -1.447 | -2.283 | 1.519 |
| Cys | 0.887 | -1.404 | -2.585 | 1.532 |
| Gln | 1.006 | -1.383 | -2.582 | 1.439 |
| Glu | 0.923 | -1.510 | -2.889 | 1.492 |
| Gly | 1.476 | -1.519 | -2.460 | 1.518 |
| His($\delta$) | 1.442 | -1.413 | -1.519 | 1.427 |
| His($\epsilon$) | 1.031 | -1.372 | -2.343 | 1.354 |
| Ile | 0.941 | -1.450 | -2.562 | 1.394 |
| Leu | 0.892 | -1.327 | -2.938 | 1.626 |
| Lys | 0.833 | -1.428 | -2.844 | 1.517 |
| Met | 0.918 | -1.396 | -2.364 | 1.497 |
| Phe | 1.554 | -1.494 | -1.818 | 1.019 |
| Pro | 1.461 | -1.274 | -1.990 | 1.553 |
| Ser | 1.031 | -1.415 | -2.557 | 1.457 |
| Thr | 1.147 | -1.241 | -2.522 | 1.733 |
| Trp | 1.535 | -1.580 | -1.149 | 0.784 |
| Tyr | 0.722 | -1.579 | -2.381 | 0.886 |
| Val | 0.984 | -1.419 | -2.531 | 1.427 |
| Average | 1.095 | -1.426 | -2.388 | 1.406 |

Table S4: Position of HOMO and LUMO energies with respect to Fermi level ($E_F$) in the interfacial gold / amino-acid models. Original GGA levels (obtained with vdW-DF) are listed together with corrected DFT+$\Sigma$ values.

| Amino acid | vdW-DF | | DFT+$\Sigma$ | |
|---|---|---|---|---|
| | HOMO | LUMO | HOMO | LUMO |
| Ala | -0.700 | 3.807 | -3.399 | 5.523 |
| Arg | -0.932 | 3.694 | -3.257 | 5.280 |
| Asn | -0.929 | 3.422 | -3.282 | 4.843 |
| Asp | -1.120 | 3.324 | -3.158 | 4.922 |
| Cys | -0.930 | 3.508 | -3.339 | 5.156 |
| Gln | -0.965 | 3.471 | -3.329 | 5.000 |
| Glu | -0.829 | 3.535 | -3.542 | 5.157 |
| Gly | -0.932 | 3.830 | -3.191 | 5.464 |
| His($\delta$) | -0.794 | 3.481 | -2.154 | 5.011 |
| His($\epsilon$) | -0.932 | 3.362 | -3.198 | 4.953 |
| Ile | -0.820 | 3.724 | -3.192 | 5.212 |
| Leu | -0.758 | 3.868 | -3.372 | 5.498 |
| Lys | -0.821 | 3.590 | -3.510 | 5.216 |
| Met | -0.923 | 3.475 | -3.648 | 4.639 |
| Phe | -1.137 | 3.301 | -2.979 | 4.525 |
| Pro | -0.917 | 3.837 | -2.714 | 5.606 |
| Ser | -1.140 | 3.668 | -3.600 | 5.262 |
| Thr | -1.145 | 3.562 | -3.570 | 5.381 |
| Trp | -0.565 | 3.095 | -1.538 | 3.934 |
| Tyr | -0.473 | 3.432 | -2.625 | 4.366 |
| Val | -0.903 | 3.739 | -3.343 | 5.341 |
| Average | -0.889 | 3.558 | -3.140 | 5.061 |

Table S5: Position of HOMO and LUMO energies with respect to Fermi level ($E_F$) in the interfacial gold / amino-acid models. Original GGA levels (obtained with PBE) are listed together with corrected DFT+$\Sigma$ values.

| Amino acid | PBE | | DFT+$\Sigma$ | |
|---|---|---|---|---|
| | HOMO | LUMO | HOMO | LUMO |
| Ala | -0.585 | 3.896 | -3.418 | 5.470 |
| Arg | -0.805 | 3.772 | -3.241 | 5.215 |
| Asn | -0.797 | 3.522 | -3.362 | 4.861 |
| Asp | -0.970 | 3.420 | -3.253 | 4.939 |
| Cys | -0.829 | 3.566 | -3.414 | 5.098 |
| Gln | -0.843 | 3.552 | -3.425 | 4.991 |
| Glu | -0.706 | 3.626 | -3.595 | 5.118 |
| Gly | -0.784 | 3.931 | -3.244 | 5.449 |
| His($\delta$) | -0.695 | 3.553 | -2.214 | 4.980 |
| His($\epsilon$) | -0.810 | 3.438 | -3.153 | 4.792 |
| Ile | -0.685 | 3.821 | -3.247 | 5.215 |
| Leu | -0.644 | 3.968 | -3.582 | 5.594 |
| Lys | -0.692 | 3.680 | -3.536 | 5.197 |
| Met | -0.812 | 3.534 | -3.176 | 5.031 |
| Phe | -1.001 | 3.342 | -2.819 | 4.361 |
| Pro | -0.795 | 3.896 | -2.785 | 5.449 |
| Ser | -1.015 | 3.739 | -3.572 | 5.196 |
| Thr | -1.008 | 3.634 | -3.530 | 5.367 |
| Trp | -0.494 | 3.158 | -1.643 | 3.942 |
| Tyr | -0.366 | 3.482 | -2.747 | 4.368 |
| Val | -0.755 | 3.825 | -3.286 | 5.252 |
| Average | -0.766 | 3.636 | -3.154 | 5.042 |

Table S6: Values of spectral density functions $\Gamma_{\mathrm{HOMO}}$ and $\Gamma_{\mathrm{LUMO}}$ characterizing electronic coupling between the HOMO / LUMO orbitals of the capped amino acids and gold states of the Au(111) surface. The functions are evaluated at Fermi energy $E_F$ using PBE and vdW-DF functionals. All values are in meV.

| Amino acid | PBE | | vdW-DF | |
|---|---|---|---|---|
| | $\Gamma_{\mathrm{HOMO}}(E_F)$ | $\Gamma_{\mathrm{LUMO}}(E_F)$ | $\Gamma_{\mathrm{HOMO}}(E_F)$ | $\Gamma_{\mathrm{LUMO}}(E_F)$ |
| Ala | 16.3 | 36.1 | 20.5 | 32.0 |
| Arg | 8.6 | 58.7 | 12.6 | 63.2 |
| Asn | 20.9 | 55.6 | 24.6 | 58.4 |
| Asp | 53.4 | 36.6 | 58.4 | 40.2 |
| Cys | 23.0 | 33.2 | 27.2 | 33.7 |
| Gln | 12.6 | 54.5 | 15.7 | 63.6 |
| Glu | 13.8 | 46.1 | 15.3 | 42.9 |
| Gly | 14.6 | 45.2 | 16.7 | 44.7 |
| His($\delta$) | 143.2 | 50.2 | 144.6 | 59.4 |
| His($\epsilon$) | 20.3 | 38.2 | 30.8 | 37.5 |
| Ile | 16.5 | 61.8 | 17.1 | 73.4 |
| Leu | 32.6 | 42.3 | 37.1 | 43.0 |
| Lys | 5.7 | 62.3 | 7.3 | 66.7 |
| Met | 21.8 | 59.3 | 15.3 | 62.5 |
| Phe | 62.5 | 112.2 | 68.4 | 101.5 |
| Pro | 105.8 | 59.3 | 124.7 | 65.4 |
| Ser | 33.5 | 49.3 | 27.6 | 56.7 |
| Thr | 82.5 | 35.6 | 80.8 | 33.2 |
| Trp | 175.8 | 105.8 | 164.0 | 107.9 |
| Tyr | 11.2 | 189.4 | 14.7 | 163.1 |
| Val | 21.9 | 37.7 | 23.6 | 41.2 |

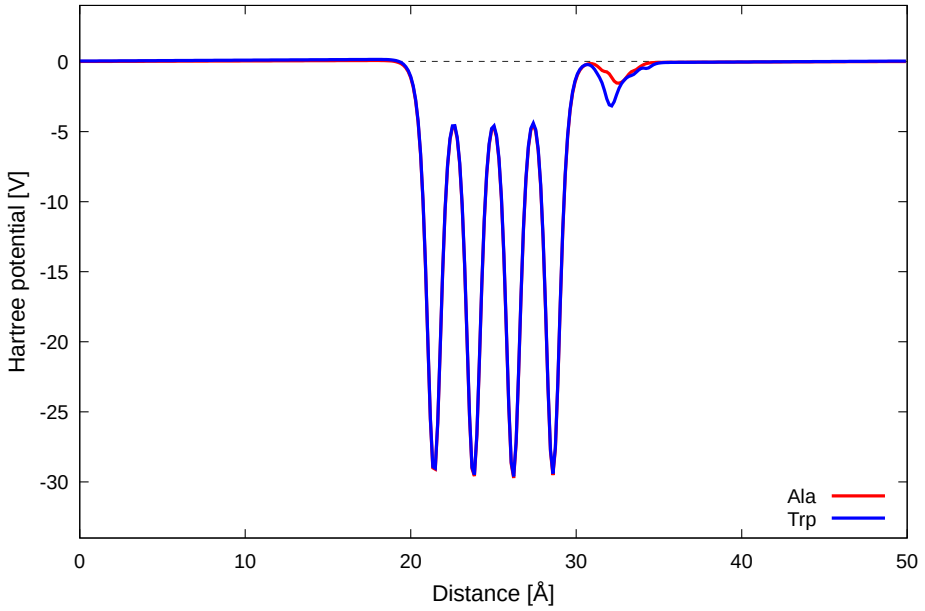


Figure S1: Hartree potential along the $z$ direction of the simulation cell (i.e. direction perpendicular to the Au(111) surface) as calculated by vdW-DF. Gold interface with alanine (Ala) and tryptophan (Trp) are compared.

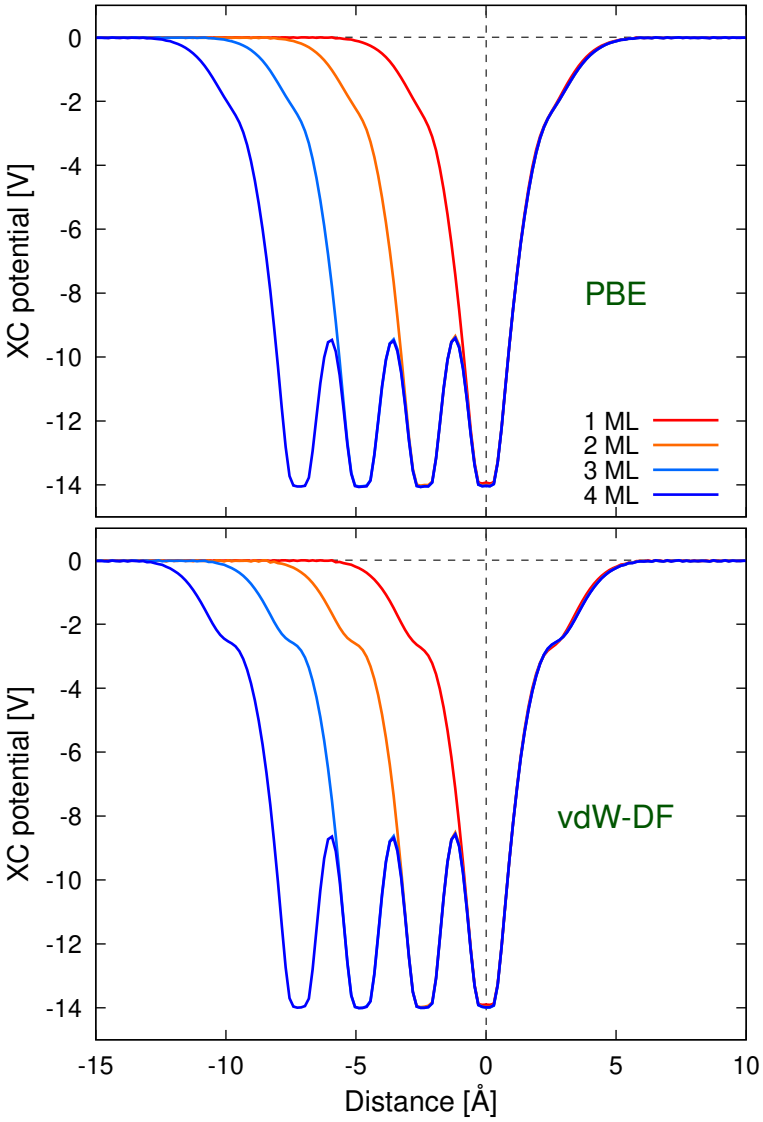


Figure S2: Plane-averaged exchange-correlation (XC) potential on the Au(111) surface as calculated in PBE and vdW-DF. The potential is plotted for 1 to 4 monolayer (ML) gold slabs. Position of the top surface layer is marked by the vertical dashed line.

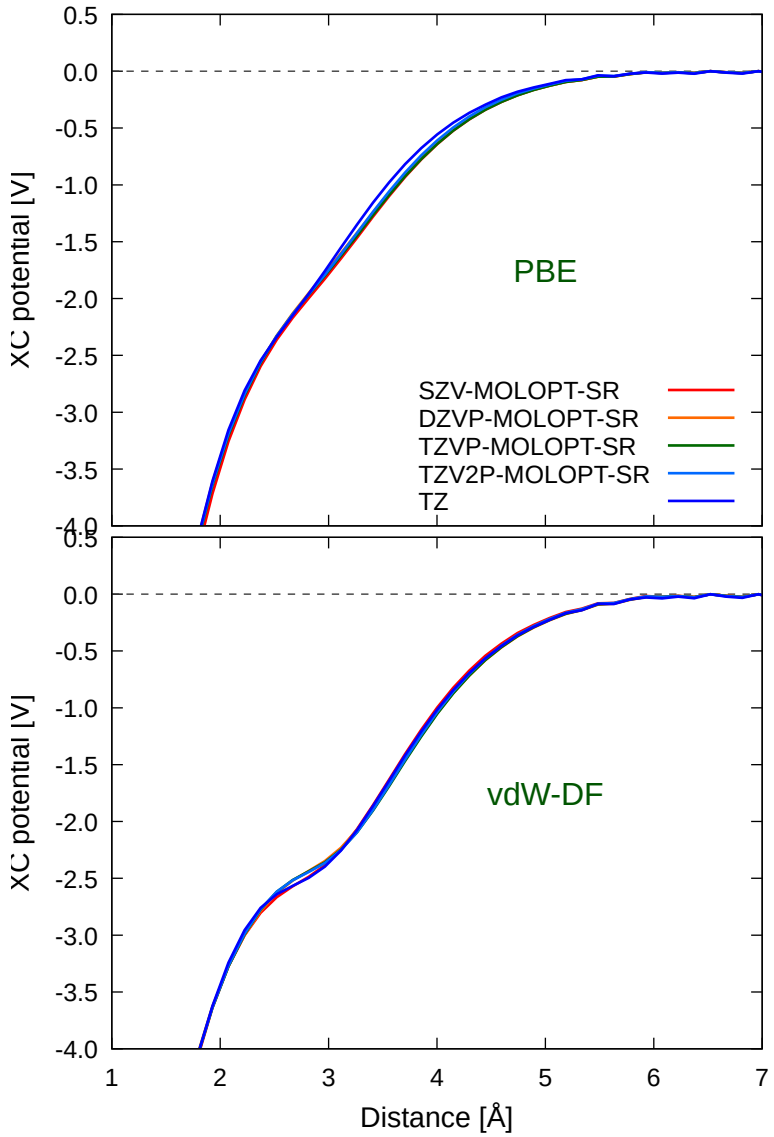


Figure S3: Plane-averaged exchange-correlation (XC) potential on the Au(111) surface as calculated in PBE and vdW-DF using different basis sets from CP2K database. Distance coordinate is calculated from the top monolayer of gold atoms.

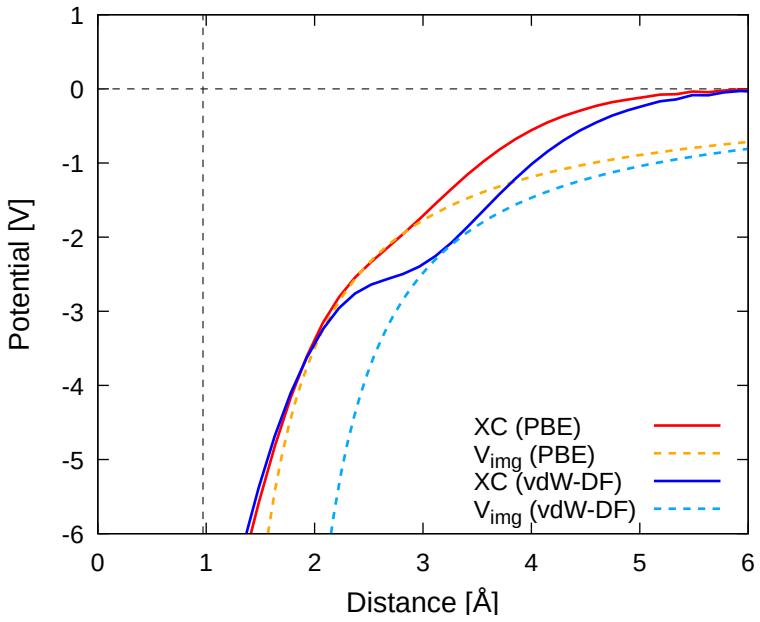


Figure S4: Classical image charge potential fitted to the exchange-correlation (XC) potential calculated by DFT on 4-layer Au(111) vacuum surface. The surface-plane position $z_0$, obtained by fitting the classical-image charge potential $V_{\mathrm{img}} \sim 1/4|z - z_0|$ to have a common tangent point with the XC potential, is located at 0.97 Å for PBE and at 1.55 Å for vdW-DF.

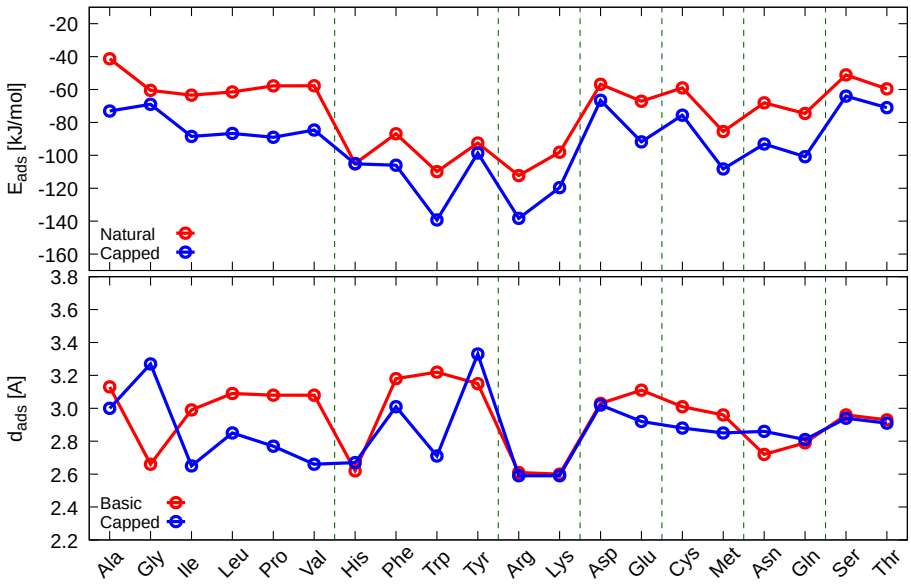


Figure S5: Adsorption energies $E_{ads}$ (given in kJ/mol) and adsorption distances $d_{ads}$ (given in Å) of natural and capped amino acids on vacuum Au (111) surface. Adsorption distances are defined as the shortest distance between the top-most gold-atom layer and the nearest amino-acid heavy atom. Vertical dashed lines indicate different groups of amino acids (aliphatic, aromatic, amines, carboxylic acids, sulfur containing, amides and hydroxylic, respectively). All data were obtained by vdW-DF.

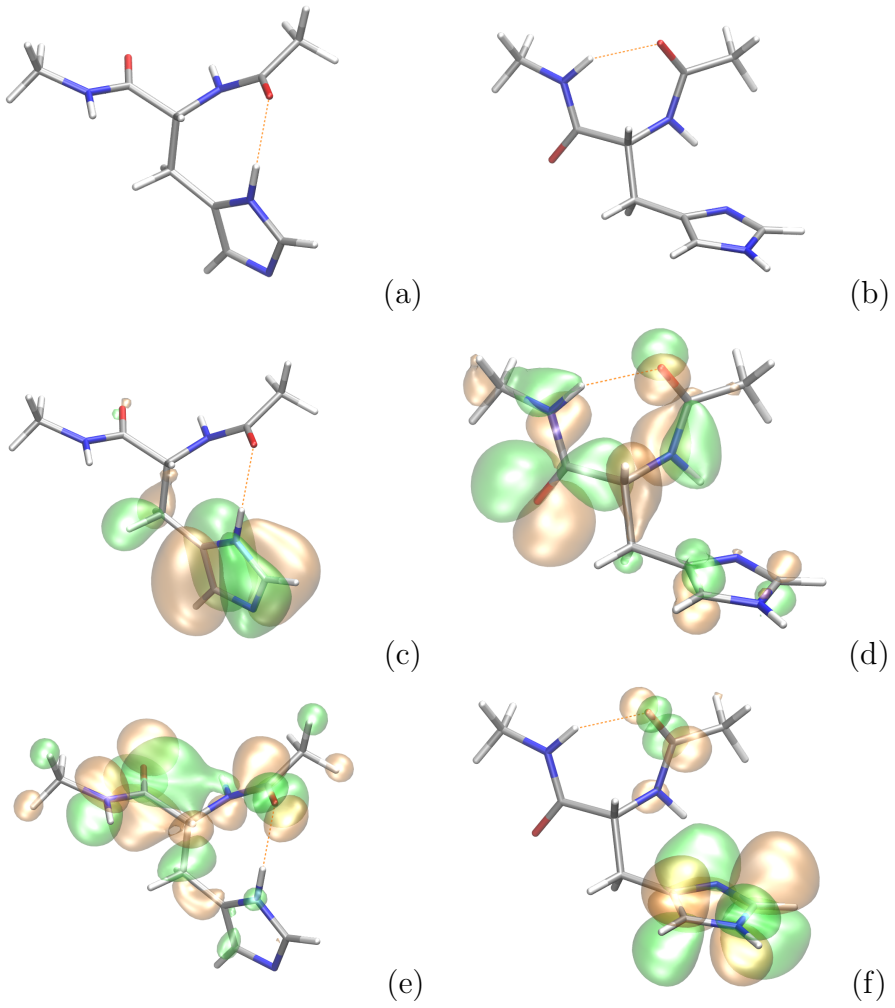


Figure S6: Gap-phase structure of the capped histidine as optimized in vdW-DF. His($\delta$) form (a) with H on the $N_\delta$ nitrogen is compared with His($\epsilon$) form (b) with H on the $N_\epsilon$ nitrogen. His($\delta$) HOMO (c) and LUMO (e) as well as His($\epsilon$) HOMO (d) and LUMO (f) are shown as green and orange isosurfaces (isovalue 0.025 au). Carbon atoms are shown in grey, nitrogen in blue and oxygen in red. Dashed orange lines indicate the H-bonding interactions.

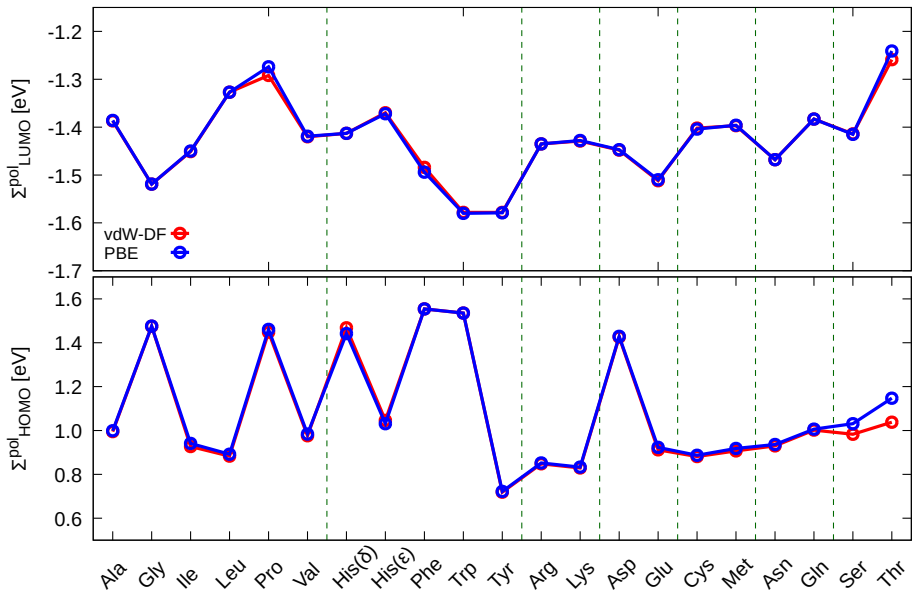


Figure S7: Renormalization frontier-orbital corrections $\Sigma^{pol}_{\mathrm{HOMO}}$ (lower panel), $\Sigma^{pol}_{\mathrm{LUMO}}$ (upper panel) obtained by integration of HOMO / LUMO amino-acid orbitals in classical image-charge interaction potential $V_{img}$. The orbitals were calculated by vdW-DF and PBE functionals on the interfacial structures optimized at vdW-DF level. Surface plane position $z_0$ = 0.97 Å obtained by $V_{img}$ fit to PBE XC potential of the clear Au(111) surface was used in all calculations. Vertical dashed lines indicate different groups of amino acids (aliphatic, aromatic, amines, carboxylic acids, sulfur containing, amides and hydroxylic, respectively).

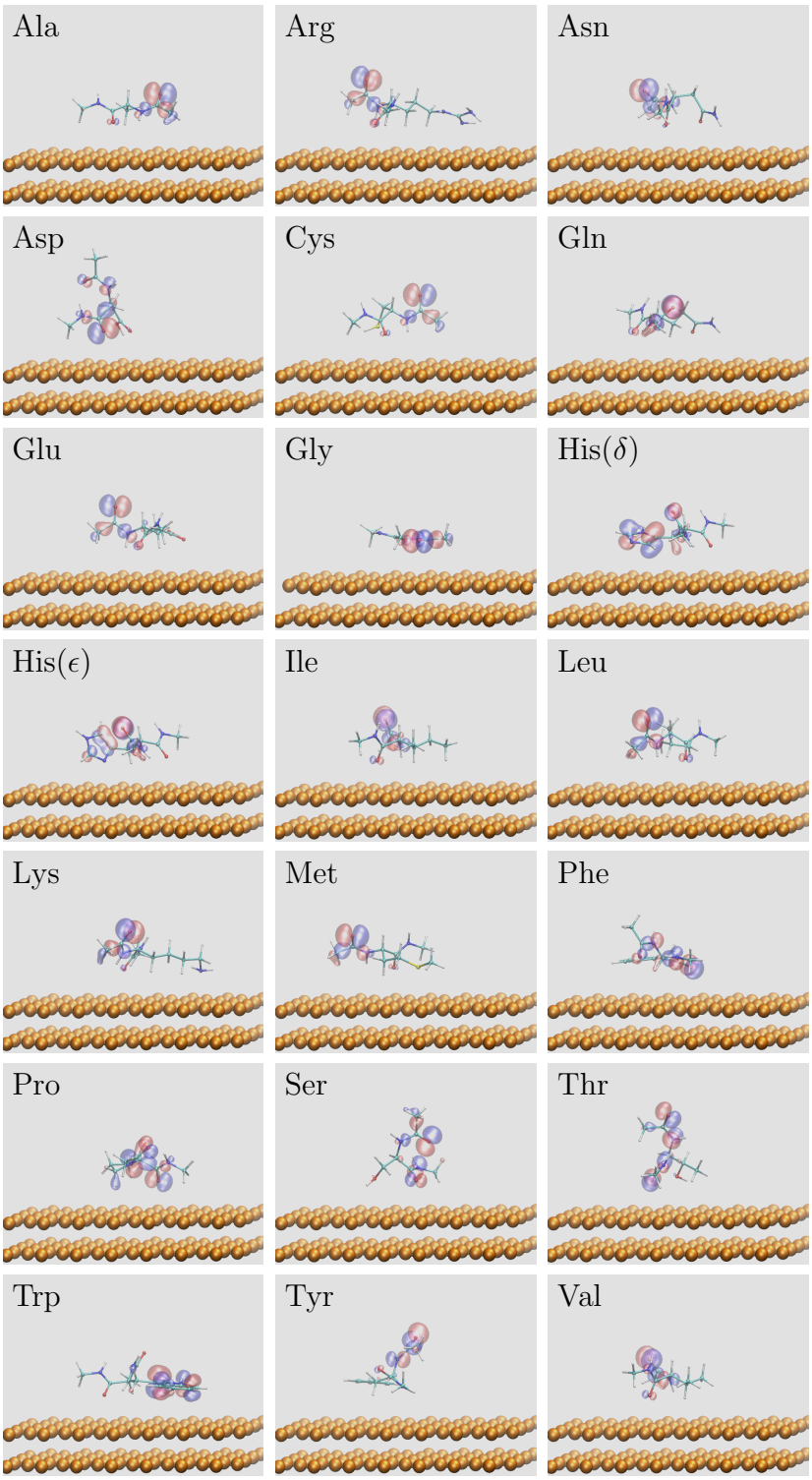


Figure S8: Highest occupied molecular orbital (HOMO) of capped amino acids adsorbed on Au(111) surface as optimized by vdW-DF.

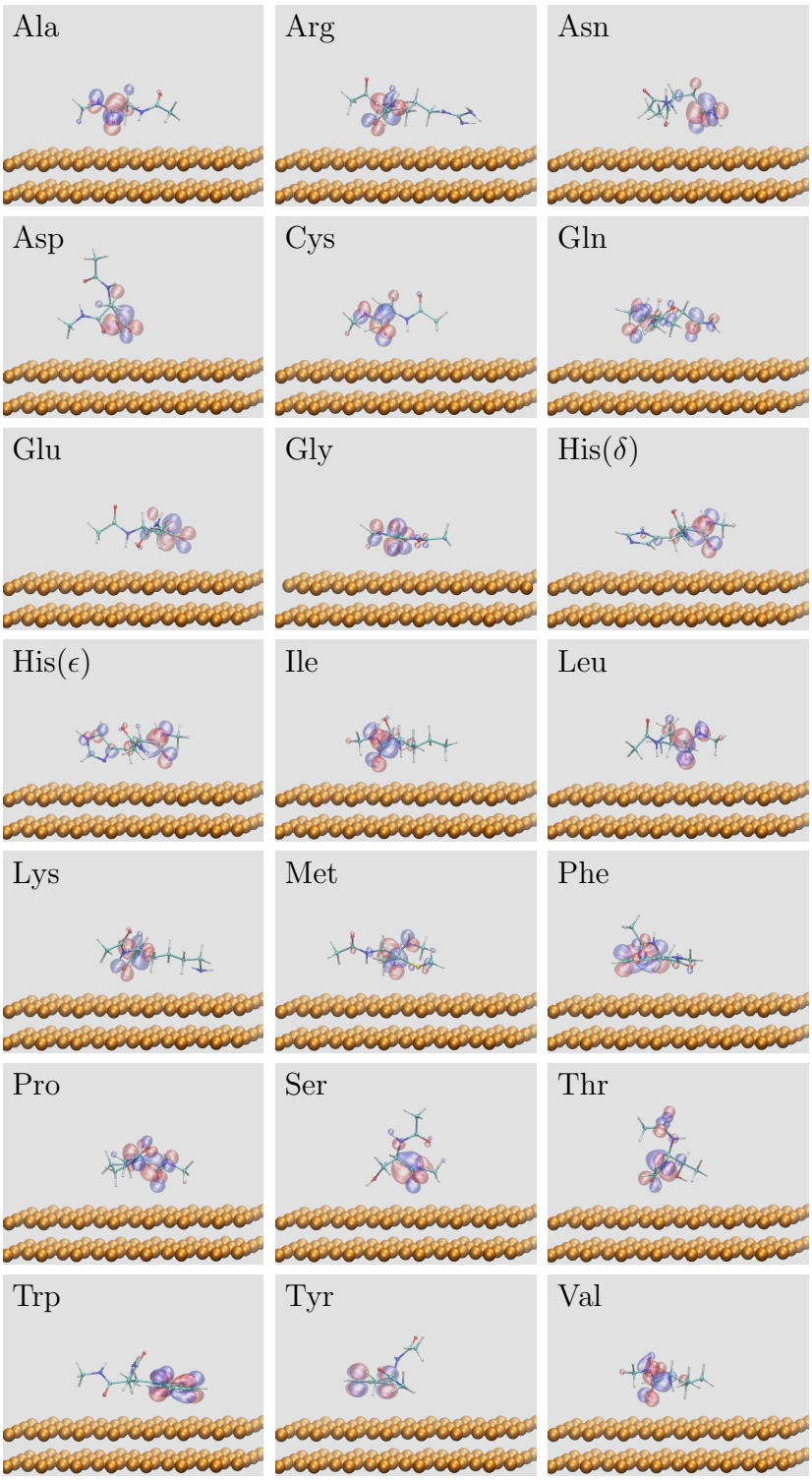


Figure S9: Lowest unoccupied molecular orbital (LUMO) of capped amino acids adsorbed on Au(111) surface as optimized by vdW-DF.

# References


(S1) Dell'Angela, M.; Kladnik, G.; Cossaro, A.; Verdini, A.; Kamenetska, M.; Tamblyn, I.; Quek, S. Y.; Neaton, J. B.; Cvetko, D.; Morgante, A.; Venkataraman, L. Relating Energy Level Alignment and Amine-Linked Single Molecule Juncition Conductance. *Nano Lett.* **2010**, *10*, 2470–2474.

(S2) Tamblyn, I.; Darancet, P.; Quek, S. Y.; Bonev, S. A.; Neaton, J. B. Electronic Energy Level Alignment at Metal-Molecule Interfaces with a GW Approach. *Phys. Rev. B* **2011**, *84*, 201402.

(S3) Biller, A.; Tamblyn, I.; Neaton, J. B.; Kronik, L. Electronic Level Alignment at a Metal-Molecule Interface from a Short-Range Hybrid Functional. *J. Chem. Phys.* **2011**, *135*, 164706.

(S4) Egger, D. A.; Liu, Z.-F.; Neaton, J. B.; Kronik, L. Reliable Energy Level Alignment at Physisorbed Molecule-Metal INterfaces from Density Functional Theory. *Nano Lett.* **2015**, *15*, 2448–2455.

(S5) Tamblyn, I. The Electronic Structure of Nanoscale Interfaces. *Mol. Simul.* **2017**, *43*, 850–860.